FEMS Microbiology Letters, 2023, **370**, 1–9
DOI: 10.1093/femsle/fnad077
Advance access publication date: 7 August 2023
Research Letter – Physiology, Biochemistry and Genetics

The phosphodiesterase RmcA contributes to the adaptation of *Pseudomonas putida* to L-arginine

Chiara Scribani-Rossi[1], María Antonia Molina-Henares[2], Simone Angeli[1], Francesca Cutruzzolà[1], Alessandro Paiardini[1], Manuel Espinosa-Urgel[2,*,†], Serena Rinaldo[1,†]

[1]Laboratory affiliated to Istituto Pasteur Italia, Fondazione Cenci Bolognetti, Department of Biochemical Sciences "A. Rossi Fanelli", Sapienza University of Rome, P.le Aldo Moro 5, 00185, Rome, Italy
[2]Department of Biotechnology and Environmental Protection, Estación Experimental del Zaidin, CSIC, Profesor Albareda, 1, Granada, 18008, Spain
*Corresponding author. Department of Biotechnology and Environmental Protection, Estacion Experimental del Zaidin, CSIC, Profesor Albareda, 1, Granada 18008, Spain. Tel: +(34) 958-181600 ext. 132; Fax: +(34) 958-129600; E-mail: manuel.espinosa@eez.csic.es
†These authors contributed equally to the work.
Editor: [Gary Rowley]

Abstract

Amino acids are crucial in nitrogen cycling and to shape the metabolism of microorganisms. Among them, arginine is a versatile molecule able to sustain nitrogen, carbon, and even ATP supply and to regulate multicellular behaviors such as biofilm formation. Arginine modulates the intracellular levels of 3′–5′cyclic diguanylic acid (c-di-GMP), a second messenger that controls biofilm formation, maintenance and dispersion. In *Pseudomonas putida*, KT2440, a versatile microorganism with wide biotechnological applications, modulation of c-di-GMP levels by arginine requires the transcriptional regulator ArgR, but the connections between arginine metabolism and c-di-GMP are not fully characterized. It has been recently demonstrated that arginine can be perceived by the opportunistic human pathogen *Pseudomonas aeruginosa* through the transducer RmcA protein (Redox regulator of c-di-GMP), which can directly decrease c-di-GMP levels and possibly affect biofilm architecture. A RmcA homolog is present in *P. putida*, but its function and involvement in arginine perceiving or biofilm life cycle had not been studied. Here, we present a preliminary characterization of the RmcA-dependent response to arginine in *P. putida* in modulating biofilm formation, c-di-GMP levels, and energy metabolism. This work contributes to further understanding the molecular mechanisms linking biofilm homeostasis and environmental adaptation.

Keywords: biofilm, c-di-GMP, arginine, metabolic reprogramming, nutrient

Introduction

Bacteria are able to behave as multicellular organisms by forming organized, surface-associated communities called biofilms, characterized by significant gene expression changes and metabolic reprogramming relative to planktonic cells to sustain the production of a protective extracellular polymeric matrix. Biofilms colonize a wide variety of surfaces including living tissue, internal medical devices, pipelines or natural aquatic systems, food processing units, and other biotic and abiotic surfaces (Donlan 2002). Hence, understanding the molecular mechanisms controlling bacterial biofilms is crucial not only for human health but also in agricultural and environmental biotechnology.

Among biofilm-forming bacteria, the plant-beneficial strain *Pseudomonas putida* KT2440 represents one of the most interesting systems, its metabolism being highly versatile for several industrial and environmental applications (Nikel and de Lorenzo 2018). These include plant growth promotion (Matilla et al. 2010, Costa-Gutiérrez et al. 2020), industrial biomanufacturing and production of synthetic and natural products, and degradation of chemical pollutants (Nikel et al. 2016, Weimer et al. 2020). Many of these applications exploit or are associated with the biofilm lifestyle (Benedetti et al. 2016).

Given the wide adaptability of *P. putida* and its potential as a chassis for sustainable chemical bioproduction, its nitrogen metabolism has attracted the interest of researchers in the context of metabolic engineering (Schmidt et al. 2022); indeed, many nitrogen sources are relevant building blocks to produce chemicals and the details of their metabolism can be used to favorably push the metabolic fluxes towards the desired product (Schmidt et al. 2022).

Among nitrogen sources, certain amino acids can influence biofilm development, and there is growing evidence that they act as environmental or metabolic signals to decide cell fate (Bernier et al. 2011). Among them, L-arginine represent a key metabolite, since it is at the crossroads of many metabolic processes, supporting bacterial growth as carbon, nitrogen, and ATP source (Scribani Rossi et al. 2022); while L-arginine fermentation is relevant to the anaerobic ATP supply in *Pseudomonas aeruginosa*, its role is less clear in *P. putida*, where overexpression of genes of the ADI pathway has been reported in response to solvent stress (Volkers et al. 2015). However, since the same conditions cause reduced ex-

Received 21 March 2023; **revised** 19 June 2023; **accepted** 27 July 2023

pression of an arginine/ornithine antiporter, these results have been interpreted as a mechanism for ornithine accumulation under stress, rather than for energy production (Volkers et al. 2015).

As a nitrogen source, L-arginine sustains the metabolism of *P. putida via* the arginine succinyltransferase (AST) and the arginine decarboxylase (ADC) pathways. As a carbon source, L-arginine is used by *P. putida via* the arginine dehydrogenase (ADH) pathway to fuel the Krebs cycle (Schmidt et al. 2022). It should be mentioned that the AST pathway, which requires succinate to yield glutamate, is presumed to be less efficient under carbon-limiting conditions.

Beyond fuel metabolism, L-arginine is involved in the production of pyoverdine, and therefore, in adaptation to oxidative stress of *P. putida* (Barrientos-Moreno et al. 2019). Not surprisingly, it is also a modulator of biofilm and c-di GMP levels in *P. putida* (Barrientos-Moreno et al. 2020), as reported for other microorganisms (Mills et al. 2015, Kumar et al. 2018, Paiardini et al. 2018). A summary of the metabolic pathways regulating arginine levels and their link to c-di-GMP is depicted in Figure S1 (Supporting Information).

In many bacteria, c-di-GMP functions as a second messenger with a key role in the transition between the motile planktonic phenotype and the sedentary biofilm lifestyle in response to environmental stimuli. Environmental cues control the intracellular levels of c-di-GMP by tuning the expression or the activity of the enzymes responsible for its turnover. Biosynthesis of this second messenger is performed by diguanylate cyclases (DCG) containing the conserved domain GGDEF, while the degradation into the pGpG linear derivative is due to phosphodiesterases (PDE) containing EAL or HD-GYP domain, the latter yielding GMP as final product (Römling et al. 2013). High c-di-GMP levels generally favor bacterial adhesion to surfaces and the establishment of biofilms, whereas low levels lead to biofilm dispersal and the switch to a motile lifestyle.

In *Pseudomonas* species, two classes of L-arginine sensors linked to biofilm signalling have been identified so far: ArgR and RmcA. The transcriptional regulator ArgR is a cytosolic repressor of arginine biosynthesis genes and acts as a positive regulator of arginine transport, thus altering c-di-GMP levels in *P. putida* through the control of cellular arginine (Barrientos-Moreno et al. 2022). On the other hand, RmcA is a sensor of periplasmic levels of this amino acid in *P. aeruginosa* (Paiardini et al. 2018). RmcA is a multidomain membrane PDE containing a periplasmic Venus Fly Trap (VFT) sensory domain recognizing L-arginine; a transmembrane helix (TM) links this periplasmic sensory portion to four PAS domains and the catalytic superdomain bearing the GGDEF-EAL tandem motif (Mantoni et al. 2018, Paiardini et al. 2018). In *P. aeruginosa* biofilm, this protein also controls colony morphogenesis (wrinkling) in response to the availability and the redox state of phenazines, redox-active compounds able to shuttle electrons in the extracellular environment; the hypothesis is that the protein should perceive the intracellular reducing power *via* a redox-sensitive mechanism far to be elucidated (Okegbe et al. 2017).

In this work, we have identified and performed a preliminary characterization of the *rmcA* homolog in *P. putida* KT2440. Biochemical and genetic data indicate that RmcA plays a role in biofilm control in this strain under certain environmental conditions, thus expanding the connections between arginine metabolism and c-di-GMP turnover.

Materials and methods

Bacterial strains, plasmids, and growth conditions

Pseudomonas putida KT2440 is a plasmid-free derivative of *P. putida* mt-2, which was isolated from a vegetable orchard in Japan and whose genome is completely sequenced (Regenhardt et al. 2002). Unless otherwise indicated, cultures were grown at 30°C (*P. putida*) or 37°C (*Escherichia coli*) under orbital shaking at 200 rpm in LB or M9 minimal medium (Sambrook et al. 1989) with 20 mM glucose as carbon source. When appropriate, antibiotics were added at the following concentrations (μg ml^{-1}): gentamycin (Gm), 50; kanamycin (Km), 25; and streptomycin (Sm), 100.

The Δ*rmcA* null mutant derivative of *P. putida* KT2440 was generated by homologous recombination, following a strategy similar to that previously reported (Barrientos-Moreno et al. 2020). Briefly, fragments corresponding to the upstream and downstream regions of the *rmcA* open reading frame (PP_0386) were amplified by overlapping PCR using Phusion high-fidelity DNA polymerase (Thermo Fisher Scientific) and oligonucleotides RMCA1 (5′-CCATCTAGATTCGCACCTGGGCGACT-3′), RMCA2 (5′-CTGGCAGTCAAAGGTCAGCGGCTTCAAGGACATGGCAGC-3′), RMCA3 (5′-GCTGACCTTTGACTGCCAGGATGGCACAGGTGCGAAACC-3′), and RMCA4 (5′-CCATCTAGAGGCTTGAGGCAGTTGGCTC-3′). The final PCR product was cloned into pCR2.1-TOPO and sequenced to ensure the absence of undesired point mutations generated during amplification. The fragment was then cloned into the suicide vector pKNG101 (Kaniga et al. 1991) and the resulting plasmid was introduced into *E. coli* CC118λ*pir*, to be then mobilized to *P. putida* KT2440 by triparental conjugation, with HB101 harboring pRK600 as a helper strain. Cointegrates were selected on M9 minimal medium with 15 mM citrate as the carbon source (to counterselect the *E. coli* strains), supplied with streptomycin. Clones were then grown on LB agar with 14% sucrose to select double homologous recombination events. The obtained null mutant was checked by PCR and further sequencing of the corresponding chromosomal region.

In parallel, a 4.6 kb fragment containing the *rmcA* gene and upstream region was amplified by PCR with oligonucleotides RMCA1 and RMCA4, digested with XbaI and cloned into pBBR1-MCS5 (Kovach et al. 1995). The resulting plasmid (pNM0386), was introduced in KT2440 and its Δ*rmcA* derivative by electroporation, using a previously described method (Enderle and Farwell 1998).

Bioreporter-based c-di-GMP quantification assays

The bioreporter plasmid pCdrA::*gfp*^{C} (Rybtke et al. 2012) was used to indirectly quantify c-di-GMP levels based on fluorescence. This plasmid harbors a fusion of the c-di-GMP-responsive promoter P_{cdrA} to *gfp*. The plasmid was introduced in *P. putida* strains by electroporation. Overnight cultures of the strains harboring the bioreporter, grown in M9 minimal medium with 15 mM citrate as carbon source, were inoculated in fresh medium to a final OD_{600} of 0.02 and distributed into 96-well black microplates (Greiner). Where indicated, L-arginine (Sigma-Aldrich) was added at a final concentration of 10 mM. Growth (OD_{660}) and fluorescence (excitation at 485 nm and emission at 515 nm) were monitored every 30 min using a Varioskan Lux microplate reader at 30°C. A shaking pulse of 10 seconds was done before each measurement. Data are indicated as gfp counts, which correspond to fluorescence values corrected by culture growth, and are the averages and standard deviations from three experiments with at least three replicas per strain.

Biofilm assays

Biofilm formation was analyzed as previously described (O'Toole and Kolter 1998) in polystyrene 48-well microtiter plates. Briefly, overnight cultures were diluted to an OD_{660} of 0.02 in fresh medium, distributed (150 μl per well), and incubated at 30°C in static conditions. At the indicated times, liquid was transferred to a new plate and planktonic growth was measured (OD_{660}). Biofilm plates were washed twice with distilled water and stained with crystal violet (0.4% v/v) for 15 min. After dye solubilization with glacial acetic acid (30% v/v), the biomass attached to the surface was quantified by measuring absorbance at 595 nm using a Tecan Sunrise™ microplate reader. Experiments were done in duplicate with four replicas per strain.

Protein expression and purification

The VFT^{pp} portion of *P. putida* RmcA (amino acid residues 21–265) was obtained from pET28b-RmcA-HisTag synthetic construct (Genescript) by PCR deletion (Hansson et al. 2008) using Q5 High-Fidelity DNA Polymerase (Biolabs). The protein was overexpressed in *E. coli* BL21 (DE3). Bacterial culture was grown at 37°C in Luria–Bertani (LB) (Sambrook et al. 1989) liquid medium supplemented with 30 μg ml^{-1} kanamycin (Sigma), at 180 rpm; at $OD_{600}\sim$ 0.8, protein expression was induced with 0.1 mM IPTG (isopropyl β-D-thiogalactoside; Sigma) and then the temperature was reduced to 16°C for 20 hours. Cells were harvested by centrifugation (40' at 12 000 rpm) and bacterial pellets were suspended in lysis buffer (50 mM HEPES pH 8, 300 mM NaCl, and 1 mM PMSF) and lysed by sonication on ice as follows: 3'' pulse, 9'' pause, for total 5 minutes of pulse, amplitude 65%, 1 cm probe (Sonics and Materials, Vibracell sonicator). Cell lysates were centrifuged 40' at 12 000 rpm and the protein was purified by affinity chromatography using a HisTrap column (GE Healthcare) loaded with Ni^{2+} and equilibrated with Buffer A (50 mM HEPES pH 8.5, 300 mM NaCl). Elution was done by increasing the imidazole concentration, and the protein eluted at 100 mM imidazole. Fractions containing pure protein were analyzed through SDS-page, collected, and the buffer was exchanged to remove imidazole by PD-10 desalting columns (GE Healthcare). Purified protein was loaded on an FPLC column (Superdex 200 26/600, GE Healthcare), eluted with buffer A using FPLC apparatus (Akta system), quantified by absorbance spectrum (VFT^{pp} ε_{280} = 1.576 mg ml^{-1}), and flash frozen in liquid nitrogen for storage at −20°C.

Seahorse XF analyzer respiratory assay

Cellular oxygen consumption rate (OCR) was measured by the extracellular flux analyzer XFe96 (Seahorse Bioscience, Houston, TX, USA) in the MOSBRI EU Infrastructure—HypACB facility at Sapienza University. The sensor cartridge for XFe Analyzer (hereinafter Seahorse), bearing 96 one-per-well oxygen probes, was hydrated at 30°C a day before the experiment, according to the manufacturer's instructions (Agilent, USA); the hydrated sensors cartridge will serve as a lid for the 96-wells cell plate, to cover the cell monolayer and to create the microchamber where the oxygen levels are measured during the experiment.

A single colony was used to inoculate 10 ml of M9∗ growth medium (M9∗ stands for M9 plus 1 mM $MgSO_4$ and 0.1 mM $CaCl_2$), supplemented with 0.5 mM $FeCl_2$ and 5 mM glucose; cells were grown overnight at 30°C, 180 rpm. The culture was then inoculated (final OD_{600} = 0.05) into 40 ml of M9∗ plus 5 mM glucose and allowed to grow at 30°C, 180 rpm until an OD_{600} = 0.2 was reached. The cultures were then diluted 1:10 (or 1:20) with sterile water and 90 μl seeded in each well of the 96-wells Seahorse cell culture plate precoated with poly-L-lysine hydrobromide (PLL) (P6282 Sigma Aldrich). Plates were centrifuged 10' at 4000 rpm to allow bacteria to adhere to the surface. After centrifugation, 90 μl of 2 × M9∗ was added in each well (to reach a 1 × medium in 180 μl of total volume). The concentration of cells used in the experiment was further verified by crystal violet assay, by looking at the OD_{600} after solubilization of the dye; the OD_{600} of the stained seeded bacteria was found to be linearly dependent on the OD_{600} of the corresponding liquid growth.

Seahorse cartridge bears four small extra loading ports for each well (4 × 96 ports) where it is possible to load a solution such as drug or nutrient or stressor; the experimental set up allows the addition of such solution(s) at certain time during the measurement. In this case, one port has been loaded with glucose or arginine or M9∗ as control and, when indicated with a cartoon syringe in the dedicated figures, each cell well was automatically supplemented with the corresponding nutrient. In detail, the nutrient supplementation during Seahorse measurements was performed by loading 20 μl of 10 × solution (50 mM glucose or100 mM arginine dissolved in M9, pH adjusted to 7) into port A of the Seahorse cartridge.

Each sample/treatment was analyzed in up to seven wells per experiment and at least two independent experiments were carried out; M9∗ controls were included into at least two wells per experiment. Data points represents the average of the replicates in a representative experiment ± SD.

Given the high oxygen consumption over the time, only the oxygen levels are reported, since the extrapolated OCR was not constant during the measurement; in this timeframe, when a microchamber is created above cells to keep the oxygen values, oxygen level transiently drops into hypoxic range thus affecting the linearity of the kinetics over the time.

Isothermal titration calorimetry assays

Isothermal titration calorimetry (ITC) experiments were carried out using an iTC200 microcalorimeter (MicroCal). VFT^{pp} was titrated with an arginine solution as follows: 1.5 μl aliquots of amino acid solution (0.6 mM, pH 8.5, in the same buffer of protein solution) injected into a 32 μM VFT^{pp} solution (300 mM NaCl, 50 mM Tris-HCl pH 8.5), with a time interval of 180 seconds between injections. ITC data were analyzed by integrating the heat exchange for each addition and normalized for the amount of injected protein; the heat exchange due to the dilution of the amino acid solution into the ITC buffer was subtracted, as normalized value, to the titration data. The heat of binding (H), stoichiometry (n), and dissociation constant (KD) were then calculated from plots of the heat evolved per mole of ligand injected versus the molar ratio of ligand to protein using the Malvern software provided by the vendor (single binding site equation). Data are the means and standard deviations of at least three experiments.

Results

Identification and characteristics of RmcA of *P. putida*

The protein sequence of RmcA of *P. aeruginosa* (RefSeq Id: WP_003113216.1), was used to identify the orthologous protein in *P. putida*, using BLAST (Altschul et al. 1990) and RefSeq as database source. A sequence 66% identical to RmcA of *P. aeruginosa* was retrieved (WP_010951734.1, encoded in locus PP_0386). As shown in Figure S2 (Supporting Information), the high sequence conservation and the identity of the key residues (Paiardini et al. 2005)

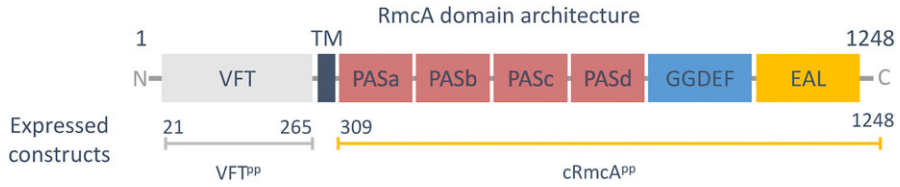

Figure 1. Domain organization of the full-length RmcA^{pp}, at the top of the panel, and the construct used for this study, including the VFT domain (cVFT^{pp}).

previously identified in RmcA of *P. aeruginosa* and necessary for catalysis (Mantoni et al. 2018) indicate that WP_010951734.1 is *bona fide* the RmcA protein from *P. putida* (hereafter, RmcA^{pp}). Domain composition analysis and modeling using PyMod 3 (Janson and Paiardini 2021) demonstrated the presence of a signal peptide (residues 1–20), a periplasmic VFT domain (Paiardini et al. 2018) comprised by residues 21–265 in RmcA^{pp}, followed by a TM helix (residues 267–286), a linker (residues 287–308), and a cytoplasmic region (residues 309–1248) composed of four PAS domains, and a GGDEF-EAL module (Fig. 1).

RmcA influences biofilm formation and c-di-GMP levels in response to arginine

A *rmcA* null mutant was constructed as described in the section "Materials and methods". No growth differences were observed between the wild type and the Δ*rmcA* mutant in the media tested (Figure S3, Supporting Information). To analyze the *in vivo* influence of RmcA on cellular c-di-GMP contents, the biosensor plasmid pCdrA-*gfp*^{C} was introduced in KT2440 and its Δ*rmcA* derivative. Cultures were inoculated in 96-well plates in liquid M9 with 15 mM citrate and with or without 10 mM arginine supplementation, and turbidity and fluorescence were monitored every 30 min in a Varioskan Lux plate as indicated in the section "Materials and methods". As reported previously (Ramos-González et al. 2016), KT2440 has physiologically low c-di-GMP levels, showing a large increase in response to arginine supplementation, leading to higher fluorescence as measured by the biosensor (Fig. 2A). This increase was enhanced in the Δ*rmcA* mutant, which otherwise shows similar fluorescence as the wild type strain in the absence of arginine, suggesting that in *P. putida* RmcA functions as an arginine-responsive PDE, as its *P. aeruginosa* counterpart. Further evidence was obtained by cloning *rmcA* in the multicopy vector pBBR1-MCS2. The resulting plasmid, pNM0386, was introduced in the wild type and the Δ*rmcA* mutant harboring pCdrA-*gfp*^{C}, and fluorescence was assayed as above, with the same strain harboring the empty vector as control. As shown in Fig. 2(B), the presence of *rmcA* in multicopy causes an overall reduction of c-di-GMP levels and the complete loss of the arginine-dependent increase. The same effect was observed in *P. putida* KT2440 harboring pNM0386 (not shown). It should be noted that under these conditions, the strains harbouring the two plasmids (pCdrA-*gfp*^{C} and either pBBR1-MCS2 or pNM0386) showed as slight reduction in their growth with respect to those harboring pCdrA-*gfp*^{C} alone (Figure S3, Supporting Information).

To determine if the influence of RmcA on c-di-GMP translates into altered biofilm dynamics, KT2440 and Δ*rmcA* strains harboring the empty vector, and the complemented Δ*rmcA* mutant, were inoculated in multiwell plates in M9 with citrate and 10 mM arginine. Biofilm formation was evaluated by staining with crystal violet and measuring absorbance after solubilization of the dye, as indicated in the section "Materials and methods". Results are shown in Fig. 2(C). Although no noticeable effect was observed in the Δ*rmcA* strain harboring the empty vector under these conditions, when the gene was present in multicopy in pNM0386, a significant reduction in attached biomass could be observed, indicating that overproduction of the protein hampers biofilm formation in *P. putida*.

The periplasmic domain of RmcA binds to arginine

Taken together, these data confirm that RmcA responds to arginine, in line with the arginine-dependent effect found in the *P. aeruginosa* counterpart (Paiardini et al. 2018). According to the bioinformatic predictions summarized to Fig. 1, the periplasmic portion of RmcA consists of a periplasmic binding protein (PBP) domain known to recognize nutrients in the periplasmic space (Felder et al. 1999). This domain is organized with a VFT fold, whose bilobate shape allows to transmit the signal by lobes closure upon nutrient binding (Felder et al. 1999). The corresponding RmcA portion (residues 21–265, hereinafter VFT^{pp}) was isolated and purified (Figure S4, Supporting Information). To verify the arginine binding, ITC assays were done, as previously reported for the *P. aeruginosa* counterpart. Microcalorimetric titrations experiments indicated that this domain binds arginine with a $K_D = 7.1 \pm 2.2$ μM, being both entropically and enthalpically favored (Fig. 3A). These data confirm that the arginine-dependent biological effect of RmcA likely involves the binding of this amino acid through its VFT motif in the periplasmic space, which in turn transmits the signal *via* the TM portion to the cytoplasmic effector.

RmcA alters the metabolic reprogramming in response to arginine

The effect of arginine as carbon source on the energy profile was evaluated using the Seahorse instrument, which allows measuring the oxygen levels and eventually the OCR in a real-time fashion. Wildtype *P. putida* and Δ*rmcA* mutant strains were tested for their ability to respond to glucose or arginine as carbon sources by tuning their respiratory activity. As reported in Fig. 3(B), the effect of glucose or arginine supplementation is comparable in sustaining the energy metabolism. On the other hand, the oxygen levels of the Δ*rmcA* strain is sensitive to the carbon source provided during the measurement (represented as a syringe cartoon in the figure) (Fig. 3C). Arginine supply sustains to a lower extent the energy metabolism as compared to the effect of glucose as carbon source. To confirm that the different effect of the two carbon sources was due to the RmcA deletion, we tested the respiratory activity of the complemented strain Δ*rmcA* pNM0386; as reported in Figure S5A (Supporting Information), respiration under arginine supplementation superposes with that measured with glucose, while the Δ*rmcA* mutant harboring the empty vector (Figure S5B, Supporting Information) was less sensitive to arginine as compared to glucose. Nevertheless, it should be mentioned that the presence of the plasmid caused an overall slowing down of

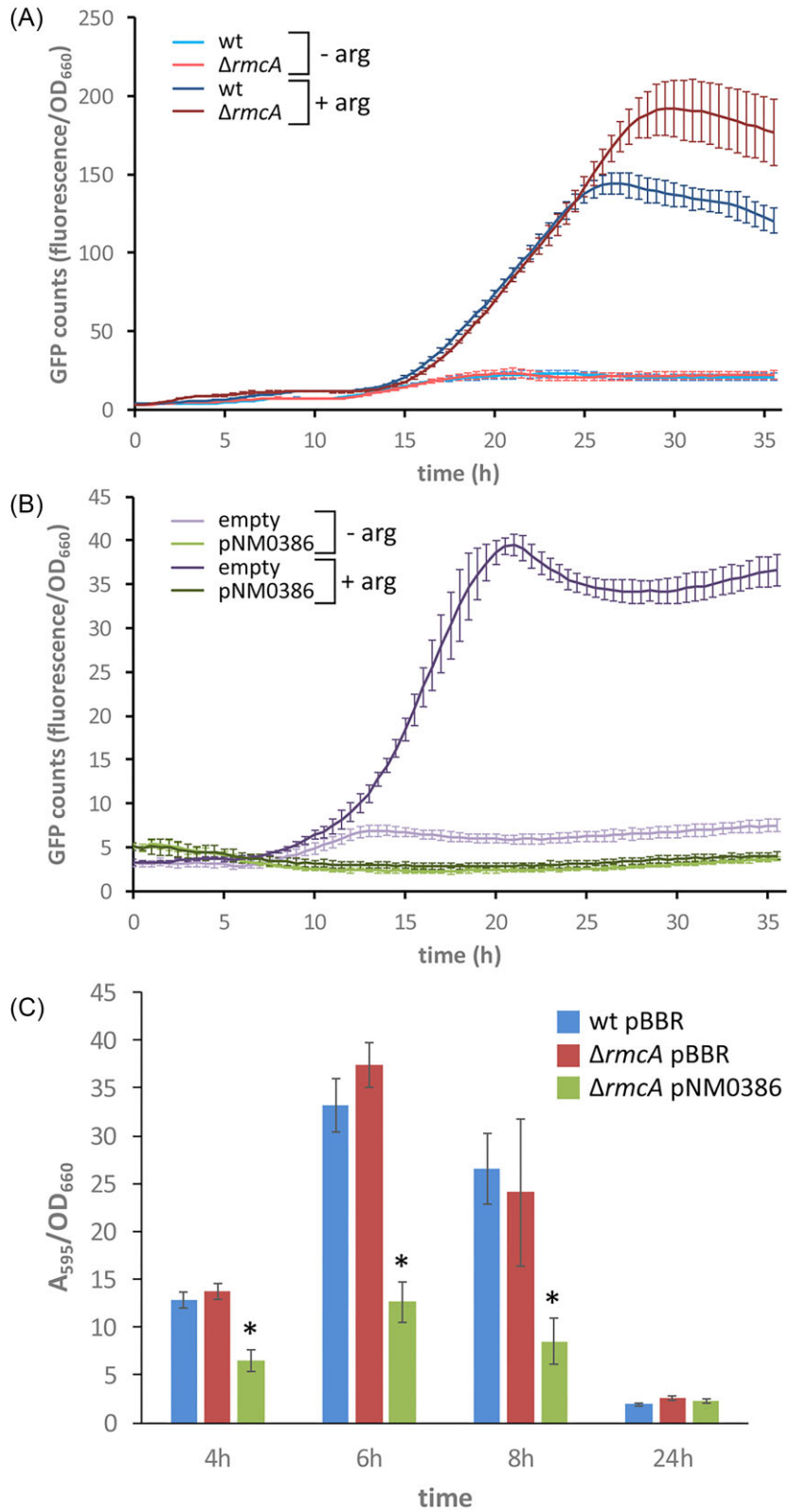

Figure 2. Influence of RmcA on c-di-GMP levels (A) and (B) and biofilm formation (C) of *P. putida*. Strains harboring pCdrA::*gfp*^{C} were inoculated in microtiter plates containing M9 + citrate with or without 10 mM arginine. (A) KT2440 (blue lines) and Δ*rmcA* (red lines); (B) Complemented Δ*rmcA* strain harboring pNM0385 (green lines) and Δ*rmcA* with the empty vector (purple lines). Fluorescence and turbidity were recorded every 30 minutes for 36 hours using a Varioskan Lux fluorimeter. Data (gfp counts) correspond to fluorescence values normalized by growth (OD_{660}) and are averages and standard deviations of one representative experiment using three experimental replicates per condition. Line color intensity indicates presence/absence of the amino acid. (C) Biofilm formation by KT2440 (blue bars) and its Δ*rmcA* derivative (red bars), harboring the empty vector (pBBR), and the complemented Δ*rmcA* strain harboring pNM0386 (green bars), during growth in 96-well polystyrene plates in static conditions. At the indicated times, planktonic growth was measured (OD_{660}) and adhered biomass was quantified after crystal violet staining (A_{595}). Data correspond to averages and standard deviations of two independent experiments with six replicates per timepoint. Statistically significant differences between KT2440 and the mutant with RmcA in multicopy are indicated (∗; Student's *t*-test, $P \leq .05$).

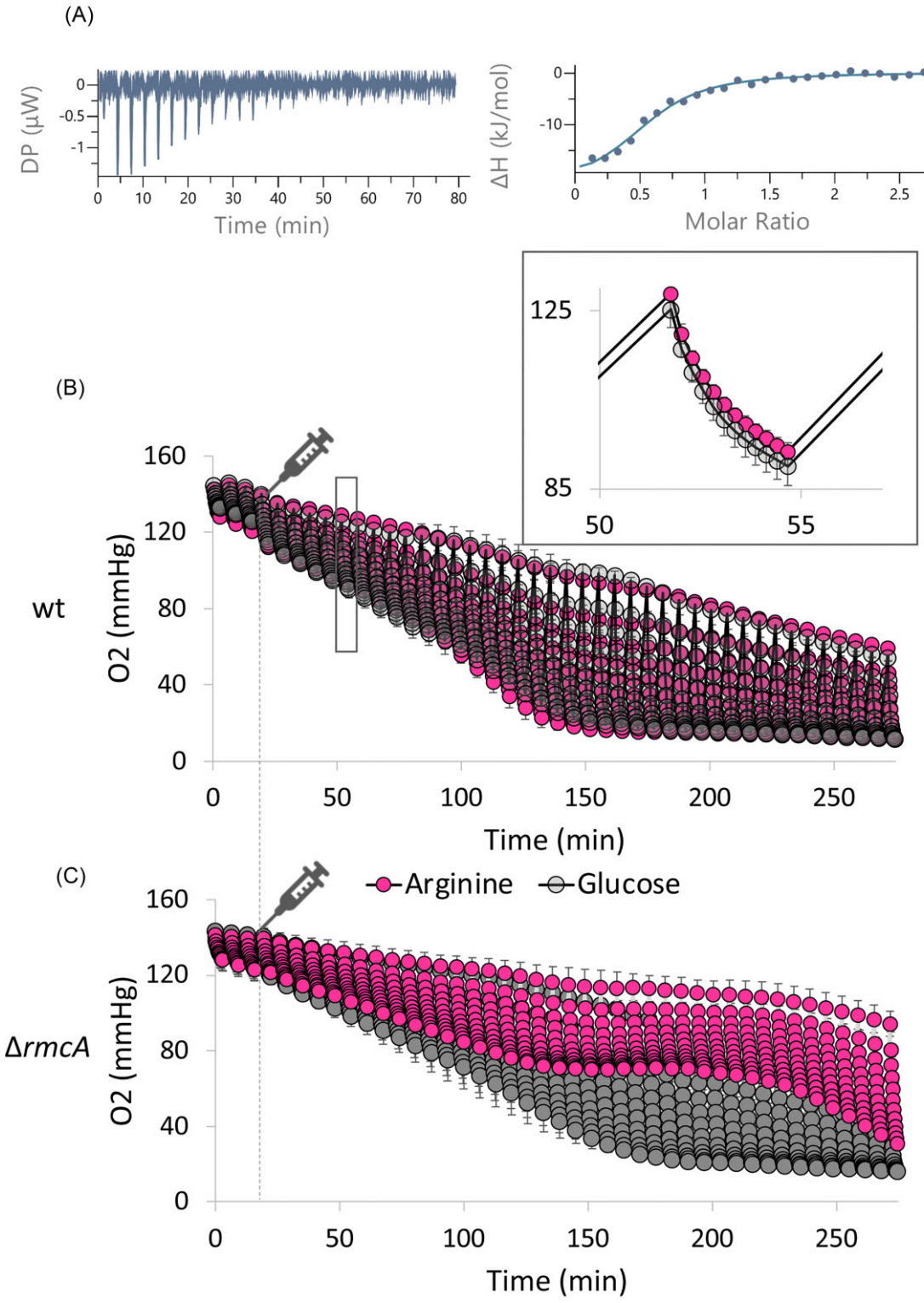

Figure 3. Arginine sensing by RmcA^{PP}. (A) Binding of L-arginine to the purified VFT fragment of RmcA, assayed by ITC. A VFT solution (32 μM) was titrated with L-arginine (600 μM in the ligand syringe) at 25°C in 20 mM Tris pH 8.5, 150 mM NaCl. The left-hand panel shows the heat exchange in time; in the right-hand panel the normalized enthalpy exchange (black squares, reported as Kcal/Mol of injectant) has been reported as a function of the molar ratio between the injectant and the macromolecule. Data were fitted with the single binding site equation with the Origin software, as provided by the vendor (continuous line), yielding the following parameters: $n = 0.59 \pm 0.04$; $K_D = 7.1 \pm 2.2$ μM; $\Delta H = -23.3 \pm 0.9$ kJ/mol; and $-T\Delta S = -6.2 \pm 1.8$ kJ mol^{-1}. (B) and (C) Effect of glucose or arginine supplementation as carbon source on the respiratory activity of *P. putida* KT2440 (B) or Δ*rmcA* mutant (C). Glucose supplemented growth were seeded and washed with the sole M9∗ medium in a Seahorse cell culture plate. The oxygen levels are reported, measured every 3 minutes alternated to 3 minutes of mixing (to promote gas exchange and restore initial oxygen levels). Dashed line and syringe cartoon indicates the time where injection of glucose or arginine was done in each well by the instrument (dark and light gray symbols, respectively). The syringe cartoon highlights that the two metabolites were added during the experiments and not present *ab initio* in the medium. Figures show representative experiments; data points are the averages and standard deviation of five replicates in each experiment. A zoom of a representative kinetics is boxed in panel (B).

respiration in both the mutant and wild type strains (Figure S5C, Supporting Information). This effect could be due to the metabolic burden of maintaining a multicopy plasmid or to the antibiotic resistance, which has been previously reported to influence central metabolism (Zhang et al. 2019, Zhou et al 2022, Pan et al. 2023).

To further confirm the arginine-dependent role of RmcA, Δ*RmcA* cultures were seeded at different densities and the oxygen levels were measured: the effect of the carbon source is widened at low cell density where arginine does not push oxygen consumption into hypoxic range (Figure S6, Supporting Information).

Therefore, the loss of *rmcA* affects the oxygen consumption of *P. putida* growing in arginine as compared to glucose, contrary to what has been reported in the wild type KT2440 strain. Based on the previously published data, indicating that the ADH pathway utilizes L-arginine as carbon source (Schmidt et al. 2022), it is possible that the arginine-dependent effect of RmcA deficiency is related to an altered tuning of this metabolic pathway.

Discussion

Pseudomonas putida has a remarkable flexibility to thrive in challenging environments thanks to its versatile metabolism and its ability to cope with different stressors (Udaondo et al. 2016, Weimer et al. 2020). This versatility makes it suitable for many biotechnological and bioremediation applications, including a growing number of biofilm-based approaches, given the adaptability and robustness of these formations (Espeso et al. 2018). The capability to fine-tune biofilm formation and stability is, therefore, key to develop large-scale biofilm-based workflows. This in turn requires a deeper knowledge of the environmental and metabolic adaptations of sessile populations, and their responses to different nitrogen, carbon and energy sources.

Here, we have presented the initial characterization of RmcA in *P. putida*, a single component system previously found to control biofilm morphology in response to environmental cues in *P. aeruginosa*. We show that this transducer can modulate c-di-GMP levels and energy metabolism in response to arginine in *P. putida*, adding a new level of complexity to the intricate connections between this amino acid and the regulatory network associated to c-di-GMP (Ramos-González et al. 2016, Barrientos-Moreno et al. 2020, 2022). RmcA in *P. aeruginosa* degrades c-di-GMP in response to arginine and reducing power (Okegbe et al. 2017, Paiardini et al. 2018), the latter being particularly relevant in the deeper layers of biofilm, where electron acceptors are limiting. In this context, RmcA controls biofilm morphology to increase the surface/volume ratio, and therefore, to buffer the possible electron imbalance due to limited electrons' acceptors availability (Jo et al. 2022). The hypothesis is that this transducer acts as rheostat rather than an ON/OFF switch (Mantoni et al. 2018).

The link between RmcA and nutrients in *P. aeruginosa* has been corroborated by multiple evidence linking this transducer to nutrient homeostasis and starvation. RmcA exerts a negative influence on expression of the type III secretion system (T3SS) genes, an effect that takes place *via* direct interaction of RmcA with CbrB (Kong et al. 2022); CbrB, as a two components partner, is involved in the maintenance of the carbon–nitrogen balance, particularly for growth on carbon sources that are energetically poorly favorable (Abdou et al. 2011). Interestingly, RmcA was found to be relevant in the maintenance of biofilm when exposed to carbon-limited conditions; the corresponding mutant forms early biofilms similar to those of the wild type strain, but fails to sustain them at later stages, and shows a susceptibility to nutrient limitation, as found in the stringent response mutant (Δ*relA* Δ*spoT*) (Katharios-Lanwermeyer et al. 2021).

In this work, we have shown that this protein modulates the response of *P. putida* to arginine in terms of c-di-GMP levels, thus confirming that this transducer is devoted to finely (or locally) tuning this second messenger to readapt the energy metabolism. In particular, we have shown that *P. putida* RmcA can control the respiratory rate in response to arginine supply, thus widening the role of c-di-GMP as regulator of the central metabolism.

Contrary to *P. aeruginosa*, the metabolism of *P. putida* KT2440 is strictly aerobic (Udaondo et al. 2016, Demling et al. 2021), although it can withstand short-term oxygen deprivation; therefore, the control of RmcA by reducing power in this cell background is not predictable and more studies must be done.

RmcA is not the sole arginine sensor able to control c-di-GMP levels in *P. putida*. It was found that the transcriptional regulator ArgR can directly perceive intracellular arginine levels and regulate the import, biosynthesis and overall cellular steady state of this metabolite; moreover, it participates in regulating the respiratory activity upon arginine supplementation and modulating c-di-GMP levels (Barrientos-Moreno et al. 2022, Scribani-Rossi et al. 2023). Therefore, arginine is a metabolite perceived as a pool in the cytoplasm and as surrounding environmental cue for controlling *P. putida* biofilm (Figure S1, Supporting Information). Although we have not detected significant changes in terms of biofilm formation the Δ*rmcA* mutant compared to the wild type under the conditions tested, overexpression of the protein does have a significant impact on biofilm development, as shown in Fig. 2. The fact that *P. aeruginosa* RmcA is involved in handling starvation during biofilm maintenance (Katharios-Lanwermeyer et al. 2021) and works as a hub for protein–protein interaction with other c-di-GMP-related proteins (Yao et al. 2023) corroborates the idea that the arginine sensing carried out by this protein finely tunes c-di-GMP rather than sustaining an all-or-nothing c-di-GMP variation. The environmental conditions in which RmcA-dependent signaling has a relevant impact on *P. putida* populations, its precise role at different stages of biofim development and under different nutrient regimes, and the connection with other regulatory elements, are aspects that still require further analysis. In this respect, it would be interesting to characterize the RmcA-mediated arginine response in genetic backgrounds defective in specific arginine-related pathways (biosynthesis, transport, or catabolism), to gain mechanistic insights into the nutrient-based control of biofilm development and stability in *P. putida*.

Acknowledgments

Francesca Romana Liberati and Giovanna Boumis are gratefully acknowledged for assistance with Seahorse experiments. Malvern and Alfatest are acknowledged for providing the software for ITC data analysis.

Supplementary data

Supplementary data is available at *FEMSLE Journal* online.

***Conflict of interest*:** The authors declare no conflict of interest.

Funding

This project has received funding from the European Union's Horizon 2020 research and innovation programme under grant agreement number 101004806 MOSBRI, DSB-

UROM TNA access provider for Seahorse experiment (to M.E.U.). Financial support from the Sapienza University of Rome (RM120172A7AD98EB to S.R. and AR12117A63EE6037, AR2221816C44C7B3 to C.S.R.), and grant PID2019-109372GB-I00 funded by MCIN/AEI/10.13039/501100011033 (M.E.U. and M.A.M.H.), are also acknowledged.

References

Abdou L, Chou HT, Haas D *et al.* Promoter recognition and activation by the global response regulator CbrB in *Pseudomonas aeruginosa*. *J Bacteriol* 2011;**193**:2784–92.

Altschul SF, Gish W, Miller W *et al.* Basic local alignment search tool. *J Mol Biol* 1990;**215**:403–10.

Barrientos-Moreno L, Molina-Henares MA, Pastor-García M *et al.* Arginine biosynthesis modulates pyoverdine production and release in *Pseudomonas putida* as part of the mechanism of adaptation to oxidative stress. *J Bacteriol* 2019;**201**:e00454–19.

Barrientos-Moreno L, Molina-Henares MA, Ramos-González MI *et al.* Arginine as an environmental and metabolic cue for cyclic diguanylate signalling and biofilm formation in *Pseudomonas putida*. *Sci Rep* 2020;**10**:13623.

Barrientos-Moreno L, Molina-Henares MA, Ramos-González MI *et al.* Role of the transcriptional regulator ArgR in the connection between arginine metabolism and c-di-GMP signaling in *Pseudomonas putida*. *Appl Environ Microbiol* 2022;**88**:e0006422.

Benedetti I, de Lorenzo V, Nikel PI. Genetic programming of catalytic *Pseudomonas putida* biofilms for boosting biodegradation of haloalkanes. *Metab Eng* 2016;**33**:109–18.

Bernier SP, Ha DG, Khan W *et al.* Modulation of *Pseudomonas aeruginosa* surface-associated group behaviors by individual amino acids through c-di-GMP signaling. *Res Microbiol* 2011;**162**:680–88.

Costa-Gutiérrez SB, Lami MJ, Santo MCC *et al.* Plant growth promotion by *Pseudomonas putida* KT2440 under saline stress: role of *eptA*. *Appl Microbiol Biotechnol* 2020;**104**:4577–92.

Demling P, Ankenbauer A, Klein B *et al.* *Pseudomonas putida* KT2440 endures temporary oxygen limitations. *Biotechnol Bioeng* 2021;**118**:4735–50.

Donlan RM. Biofilms: microbial life on surfaces. *Emerg Infect Dis* 2002;**8**:881–90.

Enderle PJ, Farwell MA. Electroporation of freshly plated *Escherichia coli* and *Pseudomonas aeruginosa* cells. *BioTechniques* 1998;**25**:954–95.

Espeso DR, Martínez-García E, Carpio A *et al.* Dynamics of *Pseudomonas putida* biofilms in an upscale experimental framework. *J Ind Microbiol Biotechnol* 2018;**45**:899–911.

Felder CB, Graul RC, Lee AY *et al.* The venus flytrap of periplasmic binding proteins: an ancient protein module present in multiple drug receptors. *AAPS PharmSci* 1999;**1**:E2.

Hansson MD, Rzeznicka K, Rosenbäck M *et al.* PCR-mediated deletion of plasmid DNA. *Anal Biochem* 2008;**375**:373–75.

Janson G, Paiardini A. PyMod 3: a complete suite for structural bioinformatics in PyMOL. *Bioinformatics* 2021;**37**:1471–72.

Jo J, Price-Whelan A, Dietrich LEP. Gradients and consequences of heterogeneity in biofilms. *Nat Rev Microbiol* 2022;**20**:593–607.

Kaniga K, Delor I, Cornelis GR. A wide-host-range suicide vector for improving reverse genetics in gram-negative bacteria: inactivation of the *blaA* gene of *Yersinia enterocolitica*. *Gene* 1991;**109**:137–41.

Katharios-Lanwermeyer S, Whitfield GB, Howell PL *et al.* *Pseudomonas aeruginosa* uses c-di-GMP phosphodiesterases RmcA and MorA to regulate biofilm maintenance. *mBio* 2021;**12**:e03384–20.

Kong W, Luo W, Wang Y *et al.* Dual GGDEF/EAL-domain protein RmcA controls the type III secretion system of *Pseudomonas aeruginosa* by interaction with CbrB. *ACS Infect Dis* 2022;**8**:2441–50.

Kovach ME, Elzer PH, Hill DS *et al.* Four new derivatives of the broad-host-range cloning vector pBBR1MCS, carrying different antibiotic-resistance cassettes. *Gene* 1995;**166**:175–76.

Kumar B, Sorensen JL, Cardona ST. A c-di-GMP-modulating protein regulates swimming motility of *Burkholderia cenocepacia* in response to arginine and glutamate. *Front Cell Infect Microbiol* 2018;**8**:56.

Mantoni F, Paiardini A, Brunotti P *et al.* Insights into the GTP-dependent allosteric control of c-di-GMP hydrolysis from the crystal structure of PA0575 protein from *Pseudomonas aeruginosa*. *FEBS J* 2018;**285**:3815–34.

Matilla MA, Ramos JL, Bakker PA *et al.* *Pseudomonas putida* KT2440 causes induced systemic resistance and changes in *Arabidopsis* root exudation. *Environ Microbiol Rep* 2010;**2**:381–88.

Mills E, Petersen E, Kulasekara BR *et al.* A direct screen for c-di-GMP modulators reveals a *Salmonella typhimurium* periplasmic L-arginine-sensing pathway. *Sci Signal* 2015;**8**:ra57.

Nikel PI, Chavarría M, Danchin A *et al.* From dirt to industrial applications: *P seudomonas putida* as a synthetic biology chassis for hosting harsh biochemical reactions. *Curr Opin Chem Biol* 2016;**34**:20–29.

Nikel PI, de Lorenzo V. *Pseudomonas putida* as a functional chassis for industrial biocatalysis: from native biochemistry to trans-metabolism. *Metab Eng* 2018;**50**:142–55.

Okegbe C, Fields BL, Cole SJ *et al.* Electron-shuttling antibiotics structure bacterial communities by modulating cellular levels of c-di-GMP. *Proc Natl Acad Sci USA* 2017;**114**:E5236–45.

O'Toole GA, Kolter R. Initiation of biofilm formation in *Pseudomonas fluorescens* WCS365 proceeds via multiple, convergent signalling pathways: a genetic analysis. *Mol Microbiol* 1998;**28**:449–61.

Paiardini A, Bossa F, Pascarella S. CAMPO, SCR_FIND and CHC_FIND: a suite of web tools for computational structural biology. *Nucleic Acids Res* 2005;**33**:W50–55.

Paiardini A, Mantoni F, Giardina G *et al.* A novel bacterial L-arginine sensor controlling c-di-GMP levels in *Pseudomonas aeruginosa*. *Proteins* 2018;**86**:1088–96.

Pan Z, Fan L, Zhong Y *et al.* Quantitative proteomics reveals reduction in central carbon and energy metabolisms contributes to gentamicin resistance in *Staphylococcus aureus*. *J Proteomics* 2023;**277**:104849.

Ramos-González MI, Travieso ML, Soriano MI *et al.* Genetic dissection of the regulatory network associated with high c-di-GMP levels in *Pseudomonas putida* KT2440. *Front Microbiol* 2016;**7**:1093.

Regenhardt D, Heuer H, Heim S *et al.* Pedigree and taxonomic credentials of *Pseudomonas putida* strain KT2440. *Environ Microbiol* 2002;**4**:912–15

Römling U, Galperin MY, Gomelsky M. Cyclic di-GMP: the first 25 years of a universal bacterial second messenger. *Microbiol Mol Biol Rev* 2013;**77**:1–52.

Rybtke MT, Borlee BR, Murakami K *et al.* Fluorescence-based reporter for gauging cyclic di-GMP levels in *Pseudomonas aeruginosa*. *Appl Environ Microbiol* 2012;**78**:5060–69.

Sambrook J, Fritsch EF, Maniatis T. *Molecular Cloning: A Laboratory Manual*. Cold Spring Harbor: Cold Spring Harbor Laboratory Press; 1989.

Schmidt M, Pearson AN, Incha MR *et al.* Nitrogen metabolism in *Pseudomonas putida*: functional analysis using random barcode transposon sequencing. *Appl Environ Microbiol* 2022;**88**:e0243021.

Scribani Rossi C, Barrientos-Moreno L, Paone A *et al.* Nutrient sensing and biofilm modulation: the example of L-arginine in *Pseudomonas*. *Int J Mol Sci* 2022;**23**:4386.

Scribani-Rossi C, Molina-Henares MA, Espinosa-Urgel M *et al.* Exploring the metabolic response of *Pseudomonas putida* to L-arginine. *FEBS J* 2023. (revised submitted).

Udaondo Z, Molina L, Segura A *et al.* Analysis of the core genome and pangenome of *Pseudomonas putida*. *Environ Microbiol* 2016;**18**:3268–83.

Volkers RJ, Snoek LB, Ruijssenaars HJ *et al.* Dynamic response of *Pseudomonas putida* S12 to sudden addition of toluene and the potential role of the solvent tolerance gene *trgI*. *PLoS ONE* 2015;**10**:e0132416.

Weimer A, Kohlstedt M, Volke DC *et al.* Industrial biotechnology of *Pseudomonas putida*: advances and prospects. *Appl Microbiol Biotechnol* 2020;**104**:7745–66.

Yao Y, Xi N, Hai E *et al.* PA0575 (RmcA) interacts with other c-di-GMP metabolizing proteins in *Pseudomonas aeruginosa* PAO1. *J Gen Appl Microbiol* 2023;**68**:232–41.

Zhang S, Wang J, Jiang M *et al.* Reduced redox-dependent mechanism and glucose-mediated reversal in gentamicin-resistant *Vibrio alginolyticus*. *Environ Microbiol* 2019;**21**:4724–39.

Zhou Y, Yong Y, Zhu C *et al.* Exogenous D-ribose promotes gentamicin treatment of several drug-resistant *Salmonella*. *Front Microbiol* 2022;**13**:1053330.

Received 21 March 2023; **revised** 19 June 2023; **accepted** 27 July 2023